The Mechanism of Burn-in Loss in a High Efficiency Polymer Solar Cell

*Craig H. Peters, I. T. Sachs-Quintana, William R. Mateker, Thomas Heumueller, Jonathan Rivnay, Rodigo Noriega, Zach M. Beiley, Eric T. Hoke, Alberto Salleo, and Michael D. McGehee**

A new class of push-pull polymers combined with a fullerene derivative in a bulk heterojunction (BHJ) architecture have enabled organic photovoltaic (OPV) efficiencies approaching 10% with the highest NREL certified efficiency now at 8.3%.[1–8] This is a significant improvement over the 5% efficiency achieved by the well-studied polymer poly(3-hexylthiophene) (P3HT) in 2005.[9] These efficiency gains have brought organic solar cells closer to commercial viability, highlighting the importance of studying the lifetime and reliability of OPV devices. The lifetime and degradation mechanisms of BHJ solar cells that employ P3HT have been well studied,[10–15] however, lifetime studies on the recently developed high performance polymers have been limited. Many of these high performance polymers generally show less structural order than the more crystalline polymer P3HT[6,16,17] and as such, may exhibit lifetimes and degradation pathways that are quite different from P3HT. Another reason to expect different behavior is that fullerenes can intercalate between the polymer sidechains of some polymers to create a molecular mixture that enables rapid exciton dissociation.[18,19] One such polymer, poly[*N*-9"-hepta-decanyl-2,7-carbazole-alt-5,5-(4′,7′-di-2-thienyl-2′,1′,3′-benzothiadiazole) (PCDTBT), achieved an efficiency of 6.1% in 2009[4] and more recently 7.2%.[20] Previous work by our group[21] on PCDTBT in BHJ composites with the fullerene derivative [6,6]-phenyl C_{70}-butyric acid methyl ester ($PC_{70}BM$) showed extrapolated lifetimes approaching 7 years for encapsulated devices, which is the longest reported lifetime for polymer solar cells and double the lifetime of P3HT:PCBM devices fabricated in a similar manner. The efficiency as a function of aging time curve (**Figure 1**) showed a severe loss in the first few hundred hours of operation followed by a remarkably stable period that lasted for the duration of the 4400 hour study. The initial efficiency loss, termed "burn-in," was shown to be primarily the result of a drop in both fill factor (FF) and open-circuit voltage (V_{oc}) and to a lesser extent the short-circuit current (J_{sc}). The physical mechanism that causes the burn-in, which results in a loss of approximately 25% of the initial efficiency, remained unclear.

Here we present a systematic study of the burn-in degradation mechanism behind PCDTBT:$PC_{70}BM$ solar cells. We show that a photochemical reaction in the photoactive layer creates states in the bandgap of PCDTBT. These sub-bandgap states increase the energetic disorder in the system, which reduces the FF, V_{oc} and to a lesser extent J_{sc}. The photochemical reactions are shown to progress rapidly when first exposed to light but subsequently decrease in occurrence, which results in the stabilization of the V_{oc} and FF.

In general, degradation can occur at the electrodes or within the photoactive layer of OPV devices. Electrodes in organic electronic devices have been shown to degrade via oxidation,[10,22,23] delamination,[23–25] de-doping[26] and interfacial organometallic chemistry.[27–31] Photoactive materials can suffer from photochemical reactions,[32–36] thermochemical reactions,[37,38] morphological changes[39,40] and impurity inclusion such as metal ion diffusion from the electrodes.[31,41–44] In the following sections we describe a systematic study of the aging of PCDTBT:$PC_{70}BM$ devices in which we deduce the probable pathway for device degradation. The studies were all performed in a nitrogen environment, under one-sun intensity with illumination provided by LG PSH07 6000K sulfur plasma lamps (to limit the amount of UV radiation) and temperatures in the 40–50 °C range, unless otherwise stated. These conditions are identical to those used in the original lifetime study of PCDTBT:$PC_{70}BM$ devices.[21]

In order to determine the effect of the electrodes and the electrode/active layer interface on the degradation mechanism of PCDTBT:$PC_{70}BM$ solar cells, devices were fabricated using five different cathode/anode combinations (**Figure 2**). Aging studies were performed and the device characteristics monitored over time. Additionally, Laser Beam Induced Current (LBIC) mapping was used to confirm that there was no failure of the encapsulation barrier.[21] The average efficiency decay for 16 solar cells of each electrode type over the first 70 h of operation is shown in Figure 2. This time period is where the majority of burn-in occurs in this system. In all cases ITO was used as the transparent conducting electrode. With the exception of the devices without calcium in the electrodes, the entire set of devices had approximately the same initial efficiency of ~5.5% (V_{oc} ~ 0.87V, FF~0.63, J_{sc} ~ 10mA/cm^2); those made without calcium had an initial power conversion efficiency ~4.5% (V_{oc} ~ 0.83V, FF ~ 0.61, J_{sc} ~ 9 mA/cm^2). The samples that employed V_2O_5 and MoO_3 had fewer sampling points but

C. H. Peters, I. T. Sachs-Quintana, W. R. Mateker, T. Heumueller, J. Rivnay, Z. M. Beiley, Prof. A. Salleo, Prof. M. D. McGehee
Department of Materials Science and Engineering
Stanford University
Stanford, CA 94305, USA
E-mail: mmcgehee@stanford.edu
R. Noriega, E. T. Hoke
Department of Applied Physics
Stanford University
Stanford, CA 94305, USA

DOI: 10.1002/adma.201103010

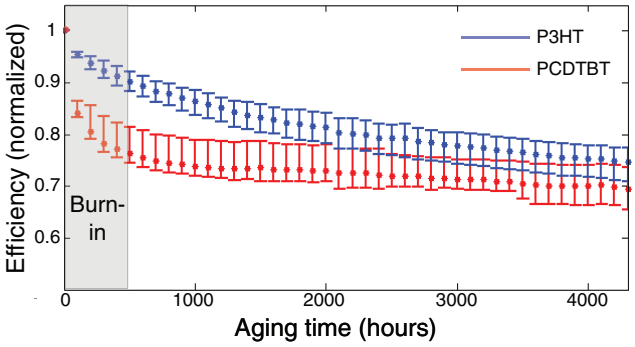

Figure 1. Efficiency decay for PCDTBT (red) and P3HT (blue) solar cells over 4400 h of continuous testing with the burn-in period shown in darkened region. The curves are each normalized by the initial value at the start of the aging process. Each point represents the average of 100 h of data for 8 solar cells of each type. The error bars show the highest and lowest values at each point.

were aged under the same conditions as the other devices. All electrode configurations led to a similar loss of efficiency. The efficiency loss in all cases was dominated by a loss of FF and V_{oc} and a small loss of J_{sc} with slight differences in the magnitude of the decay depending on the electrode used (see Supporting Information for details). Though it is possible that the cause of degradation is in the ITO or Al layers, as these were common to all devices, we will presently show that the dominant degradation process occurs in the photoactive layer.

Another factor that can significantly impact the performance of organic solar cells is the morphology of the photoactive layer.[40] Crystallite size and orientation,[45,46] π–π stacking coherence length[16,47–49] as well as interaction between the electron donating material and fullerene[50,51] are important for charge separation and transport and can change with time depending on the conditions under which the films are aged. PCDTBT has been shown to have local order in the π–π stacking direction.[16,52] Our group recently reported that when PCDTBT is

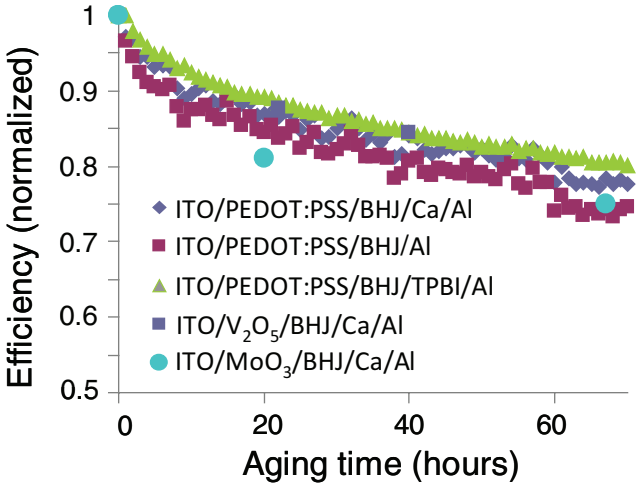

Figure 2. Efficiency loss over time for PCDTBT:$PC_{70}BM$ devices using various electrodes.

heated above its glass transition temperature, the X-ray coherence length along the π–π stacking direction decreases.[16] This shortening of the coherence length along a critical direction for charge transport is correlated with the creation of hole traps in PCDTBT and a reduction in the solar cell efficiency. In the present study, X-ray diffraction experiments were conducted to determine the effect of aging on film morphology. Films of PCDTBT were aged at 40 °C in the light for up to 200 h and GIXS patterns were obtained at beamline 11-3 at the Stanford Synchroton Radiation Lightsource. The results showed no evidence of a morphological change similar to what was seen after annealing at temperatures greater than 110 °C[16] (see Supporting Information for details), suggesting that the degradation mechanism responsible for the burn-in is not a morphological change in the structural order of the polymer. Though it is possible that the nano-scale phase separation between the polymer and fullerene is changing, we expect this change to be minimal because the polymer glass transition temperature[53] is much higher than the operating temperatures used in this study.

Chemical reactions in conjugated polymers have been well-studied because of their importance in the more mature technology of organic light-emitting diodes. In some cases LED materials degrade when excitons are present[32,54–56] and in other cases they degrade when molecules are in the charged state.[57,58] Organic semiconductors could also potentially degrade at elevated temperatures even when excitons or polarons are not present. In order to probe chemical reactions in the initial degradation of PCDTBT:$PC_{70}BM$ solar cells, the V_{oc} under 1 sun illumination was periodically measured after aging under three different experimental conditions: 1) aging at a constant temperature of 50 °C in the dark with no applied bias, 2) aging at a constant temperature of 50 °C under one-sun illumination (using a white-light LED) and operating at open-circuit and 3) forward bias in the dark at a constant current of 10 mA/cm^2, which is a typical current experienced for PCDTBT:$PC_{70}BM$ solar cells under normal operating conditions. For testing, the devices were loaded into a cryostat from inside a glovebox and subsequently held under high vacuum to remove external influences on device performance.

For the device aged at 50 °C under illumination at open-circuit conditions, we observed an immediate decay in the V_{oc}, which continued throughout the 40-hour experiment (**Figure 3**). A loss of FF and V_{oc} was observed in *I*–*V* curves taken before and after aging, similar to the behavior observed during burn-in (see Supporting Information for *I*–*V* curves). The device aged in the dark at 50 °C showed no change in open-circuit voltage and the *I*–*V* curves taken after aging were unchanged. The device with 10 mA/cm^2 of current in the dark showed no change in V_{oc} or in the *I*–*V* curves during aging. The lack of degradation while operating at a constant current in the dark suggests the degradation is mediated by excitons and not polarons. We hypothesize that the loss of V_{oc} and FF during burn-in are the results of photochemical reactions in PCDTBT that lead to degradation of the photoactive layer and adversely affect its charge transport properties.

Probing the charge transport properties of PCDTBT:$PC_{70}BM$ devices can allow for a deeper understanding of the effects of photochemical reactions on the device performance. Space-charge limited current models that use an analogue of Child's

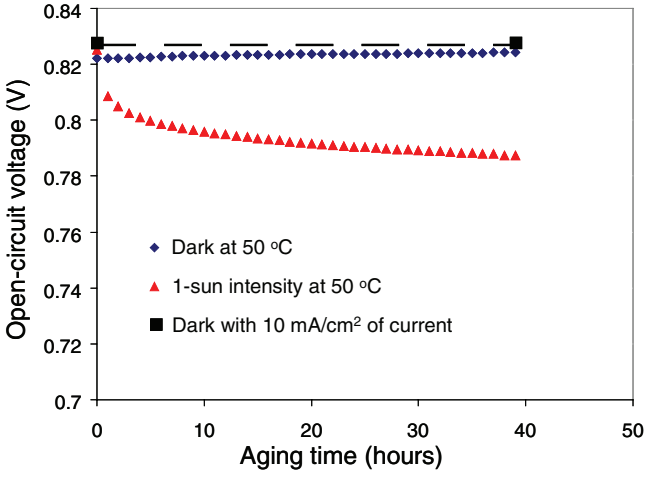

Figure 3. 1-sun intensity, open-circuit voltage (V_{oc}) of devices aged for 40 h under different conditions. The diamonds (blue) are the V_{oc} of a device held at 50 °C in the dark. The triangles (red) are the V_{oc} of a device held at 50 °C under illumination. The squares (black) are the V_{oc} of a device held in the dark with 10 mA/cm^2 of current in forward bias. The dashed line is only a guide to the eye and does not represent data points.

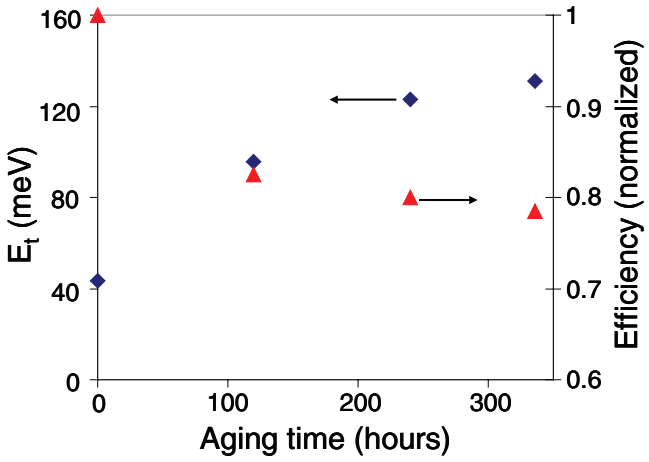

Figure 4. The diamonds (left axis) represent the characteristic width of the exponential distribution of traps (E_t) in PCDTBT:$PC_{70}BM$ hole-only diodes extending into the bandgap from the HOMO of the polymer. The hole-only diode was aged at 40 °C in a nitrogen filled box under one-sun intensity. The triangles (right axis) represent the efficiency loss of PCDTBT:$PC_{70}BM$ devices aged in a similar manner to the hole-only diodes.

Law[59] have been widely used to study the charge transport properties of conjugated polymers. However, our group has shown that current-voltage measurements made using hole-only diodes comprised of PCDTBT:$PC_{70}BM$ are not well described by Child's Law.[16] Instead, they follow a modified charge transport model that assumes an exponential distribution of trap states that extend into the bandgap and further assumes that charge carriers lying deeper in the bandgap than the Fermi level are trapped and thus immobile. This model has been used successfully to describe hole transport in organic crystals,[60] as well as electron[61–66] and hole[67–69] transport in certain conjugated polymers as a function of voltage, temperature and film thickness. By fitting the dark *I–V* curves of hole-only diodes in forward bias to this trap-mediated transport model, one can directly extract the characteristic energetic breadth of the exponential trap profile extending from the edge of the HOMO into the bandgap of the polymer. Using this model, thermal processing was shown to increase the energetic breadth of the trap distribution in PCDTBT (increasing the number of deep trap states) as a result of morphological changes.[16]

To examine trap state formation in PCDTBT:$PC_{70}BM$ due to photochemical reactions, the previously described model was used to analyze the current-voltage curves of aged PCDTBT:$PC_{70}BM$ hole-only diodes. A set of 16 identical devices were fabricated (see Experimental section) and then aged under one-sun intensity at 40 °C for over 300 hours. Throughout the aging process, the diodes were periodically loaded into a cryostat and *I-V* measurements were made in the dark at temperatures between 200–300 K in 20 K increments. Using the curve fits we determined the breadth of the exponential trap distribution (E_t) for each diode at each aging time (**Figure 4**) (see Supporting Information for curve fits). All diodes exhibited very similar results. Fresh devices exhibited an energetic trap width of ~40 meV, which is consistent with the trap width of unannealed PCDTBT:PCBM blends.[16] Over the course of aging for 350 hours, the energetic breadth of the trap distribution increased to ~130 meV. The loss of efficiency during the burn-in period from our previous report on the long term aging of PCDTBT:$PC_{70}BM$ solar cells[21] is also displayed in Figure 4. The hole trap distribution widened significantly in the first 120 h of operation (from 40 meV to 100 meV), which correlates to a loss of device efficiency of almost 18%. Over the subsequent 230 h the increase in the width of the hole trap distribution began to saturate, which corresponds well with the leveling out of the device efficiency. These results support our hypothesis of a degradation mechanism in which photochemical reactions cause an increase in the average depth of hole traps in the PCDTBT:$PC_{70}BM$ layer and result in a loss of device efficiency.

To further support our observation of the increase in states in the bandgap in aged PCDTBT:$PC_{70}BM$ films, we measured the sub-bandgap absorption. Sub-bandgap absorption features typically have low absorption coefficients[70] and their observation requires the use of sensitive measurement techniques such as photothermal deflection spectroscopy (PDS), which has been previously employed to measure absorption features in the sub-bandgap region in polymer-polymer[71] and polymer-fullerene blend films[70,72] (see Experimental Section for details on PDS measurements).

In the present study, films of PCDTBT:$PC_{70}BM$ were deposited on quartz substrates, without any electrodes present, and aged under one-sun intensity in a similar manner to the hole-only diodes previously discussed. To ensure the deflection medium (Fluorinert) did not affect the sample being tested multiple PDS spectra were taken on the same sample before aging and shown to be identical. In addition, films that were stored in the dark in nitrogen showed no change in absorption over the course of the experiment. PDS absorption spectra were periodically taken on the same region of the sample and compared (**Figure 5**). The absorption features between 0.8 and 1.1 eV have previously been attributed to the vibrational overtones of the C-H bond stretch, while absorption at energies

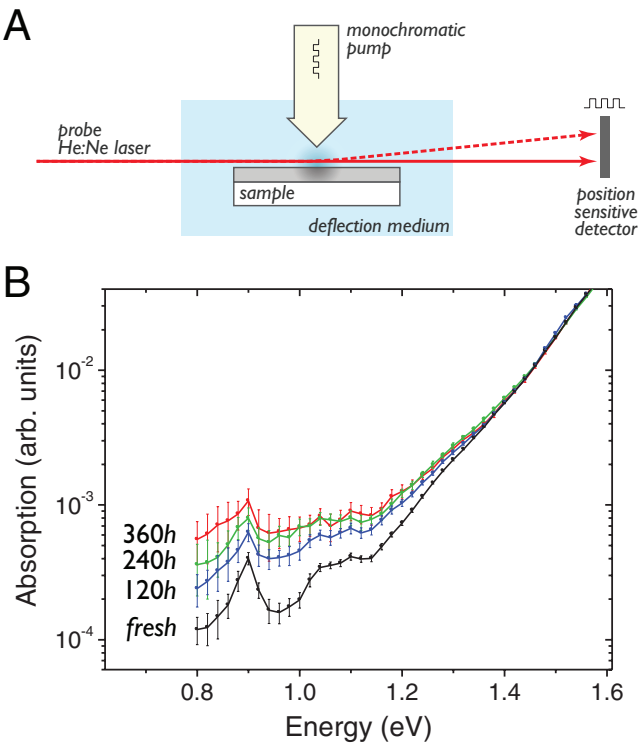

Figure 5. Photothermal deflection spectroscopy (PDS) of PCDTBT:$PC_{70}BM$ films. A) Schematic of PDS set-up. B) PDS absorption spectra of fresh and aged films; absorption below 1.3 eV increases during aging at a similar rate to the decrease in solar cell efficiency during burn-in.

above 1.2 eV is dominated by the charge-transfer state.[70] A comparison of the fresh and aged curves shows an increase in absorption in the sub-bandgap region over time. The largest increase in absorption was observed within the first 120 h of aging. The increase in sub-bandgap absorption slowed over the subsequent 240 hours. The timescale of sub-bandgap absorption increase is very similar to that of trap formation seen in hole-only diodes and efficiency decay in solar cells. The degradation seen in these films also reinforces the notion that degradation in this system is in the active layer and is independent of the choice of electrodes, since these samples were spun on bare quartz and have no electrodes.

In conclusion, PCDTBT:$PC_{70}BM$ solar cells experience a burn-in over the first 100 h of operation where up to 25% of the initial efficiency is lost, predominantly through a decrease in FF and V_{oc} and to a lesser extent the J_{sc}. The origin of the loss is a photo-induced reaction in the active layer that leads to the formation of sub-bandgap states. These states increase the energetic disorder in the active layer and may reduce device performance by a number of mechanisms, including trap-mediated recombination (i.e. Shockley-Reed-Hall recombination), reduced hole mobility and the build-up of space-charge in traps, which diminishes the electric field available to drive charge carrier separation. An important aspect of the aging process during burn-in is that it initiates rapidly but then slows down and appears to stop, suggesting that the reaction species have been depleted. While it is too early to be conclusive, it is likely that the polymer, impurities within the polymer or the chain ends photo-oxidize due to trace amounts of oxygen within the films. Evidence for the formation of hole traps upon photo-oxidation has been seen in solar cells comprised of poly(2-methoxy-5-[3′,7′-dimethyloctyloxy]-p-phenylene vinylene) (MDMO-PPV) with PCBM.[36] However, chemical reactions occurring in the fullerene are also possible with recent work out of NREL shedding some light on the role of fullerenes in the degradation process.[15] An in-depth study of the reaction pathway is necessary and currently being performed. Further investigations should help to isolate the specific reaction pathway and assist in mitigating the burn-in loss in the future, improving the commercial viability of polymer-based photovoltaic devices.

Experimental Section

Solar Cell Fabrication and Characterization: PCDTBT devices (St-Jean Photochemicals, Mw = 112 kDa) with an active area of 0.1 cm^2 were fabricated on indium tin oxide coated glass substrates (8 Ohm/sq from Thin Film Devices). The substrates were ultrasonically cleaned in detergent, acetone and isopropyl alcohol, and subsequently dried overnight in an oven at 110 °C. The substrates were placed in a UV ozone chamber for 20 min prior to the deposition of the anode. Each substrate contained 5 active devices. Films of poly(3,4-ethylenedioxythiophene) poly(styrenesulfonate) (PEDOT,CLEVIOS P VP AI 4083, work function ~5.0 eV) were deposited via spin-casting (4000 RPM for 45 sec) from aqueous solution to a thickness of 25 nm. The substrates were annealed for 10 min at 140 °C in air and then transferred into a nitrogen-filled glove box (oxygen and moisture content <3 ppm) to deposit the active layer and counter electrode. Vanadium oxide (V_2O_5, Sigma-Aldrich 99.99% purity) and molybdenum oxide (MoO_3, Alfa Aesar 99.95% purity) were thermally evaporated with a thickness of ~7 nm. For the active layer, a solution containing a mixture of PCDTBT:$PC_{70}BM$ (1:4, by weight) (from St. Jean Photochemicals and Nano-C, respectively) in 1,2-ortho–dichlorobenzene with a concentration of 25 mg ml^{-1}. The solution was stirred overnight at 90 °C then cooled to 60 °C before depositing the active layer by spin coating at a spin speed of 1500rpm for 45 s to achieve an active layer thickness of ~80 nm. The film was slowly dried overnight in a covered Petri dish in the glove box. Finally the cathode a Ca/Al (7 nm/100 nm) was deposited by thermal evaporation in a vacuum of about 1×10^{-6} mbar. In the case where 2,2′,2″-(1,3,5-benzenetriyl)tris-[1-phenyl-1H-benzimidazole] (TPBI) was used in place of Ca, a 10 nm layer of TPBI was thermal deposited at 1×10^{-6} mbar prior to the deposition of the Al cathode. Solar cells were encapsulated in a glass-on-glass architecture and aged under the sulfur plasma lamps as previously described.[21]

2D-GIXD Sample Preparation and Analysis: Films of PCDTBT were spin coated onto silicon substrates using the same method as for solar cells. The solution contained 7 mg mL^{-1} of PCDTBT in 1,2-ortho–dichlorobenzene. X-ray diffraction was performed at the Stanford Synchrotron Radiation Lightsource (SSRL) on beam line 11-3 (2-D scattering with an area detector, MAR345 image plate, at grazing incidence) with an incident energy of 12.7 keV. For grazing incidence experiments, the incidence angle was slightly larger than the critical angle, ensuring that we sampled the full film depth. Scattering data are expressed as a function of the scattering vector $q = (4\pi/\lambda)\sin\theta$ where θ is half the scattering angle and λ is the wavelength of the incident radiation. Here q_{xy} (q_z) is the component of the scattering vector parallel (perpendicular) to the substrate. Analysis of the 2D-GIXD patterns was performed with the software WxDiff provided by S.C.B. Mannsfeld.[73]

Hole-Only Diode Sample Preparation and Testing: Glass substrates coated with patterned tin-doped indium oxide (8 Ω/sq from Thin Film Devices) were cleaned and treated in a similar manner to solar cells. An aqueous solution of PEDOT:PSS was spun on top, then baked on a hotplate for 15 min at 140 °C to drive off any remaining solvent, resulting in a 25 nm film. The substrates were then transferred to a dry nitrogen glove box for the active layer deposition. The devices were fabricated on six separate

substrates with up to five active devices per substrate to ensure at least 16 active devices throughout the entirety of the experiment.

Active layer solutions were prepared in the glove box by dissolving a 1:4 weight ratio of PCDTBT: $PC_{70}BM$ in 1,2-ortho–dichlorobenzene in a concentration of 35 mg mL^{-1}. The solutions were stirred overnight at 90 °C then cooled to 60 °C before depositing the active layer by spin coating at a spin speed of 700 rpm for 45 s. Films were allowed to dry slowly in covered Petri dishes at room temperature. A top contact of CA-1914 (Plextronics, diluted by 50% in ethanol, work function of ~5.5 eV) was spin-cast in air in the dark, and the remaining solvent was driven off by heating on a hotplate at 65 °C for 15 min. Following deposition of the CA-1914, the hole-only devices were held under vacuum in an antechamber for 30 min prior to being returned to the glove box where 200 nm of Al was deposited by thermal evaporation. The area for all hole-only devices was 0.1 cm^2. To ensure that exposure to oxygen in the dark during the deposition of CA-1914 did not introduce new degradation phenomena, solar cells were fabricated and exposed to the same conditions as the hole-only diodes prior to cathode deposition. Aging of these solar cells along with solar cells that were not exposed to oxygen prior to cathode deposition showed identical burn-in behavior.

Hole-only diodes were loaded into an airtight aluminum chamber with a glass window inside a nitrogen filled glovebox and subsequently aged under sulfur plasma lamps with one-sun light intensity. Current–voltage characteristics for hole-only devices were measured in an evacuated, liquid nitrogen cooled Janus ST-100 cryostat using a Keithley 2400 source meter. Devices were loaded into the cryostat in the glove box prior to measurement to avoid exposure to air. The voltages shown in plots of hole-only current measurements in the Supporting Information were corrected for the potential lost due to series resistance, $V = V_{applied} - I \cdot R_{series}$. They were not corrected for any built-in potential due to a difference in electrode work functions, because in the measurement range (3–15 V) this correction is small, and the actual built in voltage is not necessarily the difference in nominal electrode work functions.

Photothermal Deflection Spectroscopy: PDS relies on the complete or fractional conversion of absorbed electromagnetic radiation by the material of interest into heat via nonradiative de-excitation processes. This conversion process causes a temperature rise in the material itself and its surroundings. The sample to be studied is submerged in an inert fluid (Fluorinert) with a very large change in refractive index as a function of temperature, so that a small amount of heat leads to a localized change in the index of refraction in the liquid. Such change in refraction index is measured and correlated with the absorption coefficient of the material of interest. During a measurement, a modulated monochromatic pump beam (arranged perpendicular to the plane of the substrate) is absorbed by the sample. A second (transverse) probe laser beam is deflected by the localized change in the refractive index of the surrounding deflection medium, and a position sensitive detector records the periodic deflection by a lock-in technique. The measured deflection is proportional to the absorption coefficient of the measured thin film.

In the present study, films of PCDTBT:$PC_{70}BM$ were fabricated by drop casting from the same solution as that used for solar cell fabrication on quartz substrates and allowed to dry for 5 days in a glovebox. Films were then held under low vacuum for up to 2 h to further remove any remaining solvent. Films were then immersed in a cuvette filled with Fluorinert (3M). The pump beam used in PDS was obtained from a halogen lamp, then monochromated and focused onto the sample. The probe beam is a commercial He:Ne laser, and the deflection signal is measured with a position sensitive detector. Absorption measurements were then made as previously described by Goris et al.[70] For a typical time constant of 10 s in the detection lock-in amplifier 30 measurements are made for each energy; the plots show the average value with the error bars representing the standard deviation.

Supporting Information

Supporting Information is available from the Wiley Online Library or from the author.

Acknowledgements

This publication was supported by the Center for Advanced Molecular Photovoltaics (Award No KUS-C1-015-21), made by King Abdullah University of Science and Technology (KAUST). We are grateful to Plextronics for their assistance in device fabrication and guidance with performing lifetime studies. We thank St-Jean Photochemicals for providing the polymer (PCDTBT) and LG for their support in providing the sulfur plasma lamps. Additional support provided for Z.M.B. by the National Defense Science and Engineering Graduate Fellowship, for E.T.H. by the Fannie and John Hertz Foundation, for T.S.Q. and J.R. by the National Science Foundation Graduate Research Fellowship and for C.H.P. by the Stanford Graduate Fellowship.

Received: August 5, 2011
Revised: September 13, 2011
Published online: October 11, 2011

[1] Y. Liang, Z. Xu, J. Xia, S. T. Tsai, Y. Wu, G. Li, C. Ray, L. Yu, *Adv. Mater.* **2010**, *22*, E135.
[2] M. A. Green, K. Emery, Y. Hishikawa, W. Warta, *Prog. Photovoltaics: Res. Appl.* **2010**, *18*, 346.
[3] H.-Y. Chen, J. Hou, S. Zhang, Y. Liang, G. Yang, Y. Yang, L. Yu, Y. Wu, G. Li, *Nat. Photon.* **2009**, *3*, 649.
[4] S. H. Park, A. Roy, S. Beaupré, S. Cho, N. Coates, J. S. Moon, D. Moses, M. Leclerc, K. Lee, A. J. Heeger, *Nat. Photon.* **2009**, *3*, 297.
[5] R. Qin, W. Li, C. Li, C. Du, C. Veit, H.-F. Schleiermacher, M. Andersson, Z. Bo, Z. Liu, O. Inganäs, U. Wuerfel, F. Zhang, *J. Am. Chem. Soc.* **2009**, *131*, 14612.
[6] C. Piliego, T. W. Holcombe, J. D. Douglas, C. H. Woo, P. M. Beaujuge, J. M. J. Fréchet, *J. Am. Chem. Soc.* **2010**, *132*, 7595.
[7] C. M. Amb, S. Chen, K. R. Graham, J. Subbiah, C. E. Small, F. So, J. R. Reynolds, *J. Am. Chem. Soc.* **2011**, *133*, 10062.
[8] PVTech, http://www.pv-tech.org/news/nrel_validates_konarkas_8.3_power_plastic_efficiency_record **2010**.
[9] W. Ma, C. Yang, X. Gong, K. Lee, A.J. Heeger, *Adv. Func. Mater.* **2005**, *15*, 1617.
[10] M. T. Lloyd, D. C. Olson, P. Lu, E. Fang, D. L. Moore, M. S. White, M. O. Reese, D. S. Ginley, J. W. P. Hsu, *J. Mater. Chem.* **2009**, *19*, 7638.
[11] R. De Bettignies, J. Leroy, M. Firon, C. Sentein, *Synth. Met.* **2006**, *156*, 510.
[12] J. A. Hauch, P. Schilinsky, S. A. Choulis, R. Childers, M. Biele, C. J. Brabec, *Sol. Energy Mater. Sol. Cells* **2008**, *92*, 727.
[13] M. O. Reese, A. J. Morfa, M. S. White, N. Kopidakis, S. E. Shaheen, G. Rumbles, D. S. Ginley, *Sol. Energy Mater. Sol. Cells* **2008**, *92*, 746.
[14] C. Lungenschmied, G. Dennler, H. Neugebauer, N. S. Sariciftci, M. Glatthaar, T. Meyer, A. Meyer, *Sol. Energy Mater. Sol. Cells* **2007**, *91*, 379.
[15] M. O. Reese, A. M. Nardes, B. L. Rupert, R. E. Larsen, D. C. Olson, M. T. Lloyd, S. E. Shaheen, D. S. Ginley, G. Rumbles, N. Kopidakis, *Adv. Funct. Mater.* **2010**, *20*, 3476.
[16] Z. M. Beiley, E. T. Hoke, R. Noriega, J. Dacuña, G. F. Burkhard, J. A. Bartelt, A. Salleo, M. F. Toney, M. D. McGehee, *Adv. Energy Mater.* **2011**, *1*, 954.
[17] Y. Liang, L. Yu, *Acc. Chem. Res.* **2010**, *43*, 1227.
[18] A. C. Mayer, M. F. Toney, S. R. Scully, J. Rivnay, C. J. Brabec, M. Scharber, M. Koppe, M. Heeney, I. McCulloch, M. D. McGehee, *Adv. Funct. Mater.* **2009**, *19*, 1173.
[19] M. Tong, N. E. Coates, D. Moses, S. Beaupré, M. Leclerc, A. J. Heeger, *Phys. Rev. B* **2010**, *81*, 125210.
[20] Y. Sun, C. J. Takacs, S. R. Cowan, J. H. Seo, X. Gong, A. Roy, A. J. Heeger, *Adv. Mater.* **2011**, *23*, 2226.

[21] C. H. Peters, I. T. Sachs-Quintana, J. P. Kastrop, S. Beaupre, M. Leclerc, M. D. McGehee, *Adv. Energy Mater.* **2011**, *1*, 491.
[22] L. M. Do, E. M. Han, Y. Niidome, M. Fujihira, T. Kanno, S. Yoshida, A. Maeda, A. J. Ikushima, *J. Appl. Phys.* **1994**, *76*, 5118.
[23] M. Schaer, F. Nüesch, D. Berner, W. Leo, L. Zuppiroli, *Adv. Funct. Mater.* **2001**, *11*, 116.
[24] S. Gardonio, L. Gregoratti, P. Melpignano, L. Aballe, V. Biondo, R. Zamboni, M. Murgia, S. Caria, M. Kiskinova, *Org. Electron.* **2007**, *8*, 37.
[25] M. T. Lloyd, C. H. Peters, A. Garcia, I. V. Kauvar, J. J. Berry, M. O. Reese, M. D. McGehee, D. S. Ginley, D. C. Olson, *Sol. Energy Mater. Sol. Cells* **2011**, *95*, 1382.
[26] J.-S. Kim, P. K. H. Ho, C. E. Murphy, N. Baynes, R. H. Friend, *Adv. Mater.* **2002**, *14*, 206.
[27] T. Kugler, M. Logdlund, W. R. Salaneck, *IEEE J. Sel. Top. Quantum Electron.* **1998**, *4*, 14.
[28] A. M. Hawkridge, J. E. Pemberton, *J. Am. Chem. Soc.* **2003**, *125*, 624.
[29] R. J. Davis, J. E. Pemberton, *J. Am. Chem. Soc.* **2009**, *131*, 10009.
[30] Y. Gao, *Acc. Chem. Res.* **1999**, *32*, 247.
[31] T. P. Nguyen, J. Ip, P. Jolinat, P. Destruel, *Appl. Surf. Sci.* **2001**, *172*, 75.
[32] M. Yan, L. J. Rothberg, F. Papadimitrakopoulos, M. E. Galvin, T. M. Miller, *Phys. Rev. Lett.* **1994**, *73*, 744.
[33] B. H. Cumpston, K. F. Jensen, *Synth. Met.* **1995**, *73*, 195.
[34] A. Rivaton, S. Chambon, M. Manceau, J.-L. Gardette, N. Lemaître, S. Guillerez, *Polym. Degrad. Stab.* **2010**, *95*, 278.
[35] M. Manceau, E. Bundgaard, J. E. Carlé, O. Hagemann, M. Helgesen, R. Søndergaard, M. Jørgensen, F. C. Krebs, *J. Mater. Chem.* **2011**, *21*, 4132.
[36] R. Pacios, A. J. Chatten, K. Kawano, J. R. Durrant, D. D. C. Bradley, J. Nelson, *Adv. Funct. Mater.* **2006**, *16*, 2117.
[37] M. Manceau, A. Rivaton, J.-L. Gardette, S. Guillerez, N. Lemaître, *Polym. Degrad. Stab.* **2009**, *94*, 898.
[38] S. Chambon, A. Rivaton, J.-L. Gardette, M. Firon, *Polym. Degrad. Stab.* **2011**, *96*, 1149.
[39] X. Yang, J. K. J. van Duren, R. A. J. Janssen, M. A. J. Michels, J. Loos, *Macromolecules* **2004**, *37*, 2151.
[40] J. K. J. van Duren, X. Yang, J. Loos, C. W. T. Bulle-Liewma, AXeval, J. C. Hummelen, R. A. J. Janssen, *Adv. Func. Mater.* **2004**, *14*, 425.
[41] F. J. Esselink, G. Hadziioannou, *Synth. Met.* **1995**, *75*, 209.
[42] C. W. T. Bulle-Lieuwma, W. J. H. van Gennip, J. K. J. van Duren, P. Jonkheijm, R. A. J. Janssen, J. W. Niemantsverdriet, *Appl. Surf. Sci.* **2003**, *203*, 547.
[43] F. C. Krebs, K. Norrman, *Prog. Photovoltaics* **2007**, *15*, 697.
[44] M. P. de Jong, D. P. L. Simons, M. A. Reijme, L. J. van IJzendoorn, A. W. Denier van derGon, M. J. A. de Voigt, H. H. Brongersma, R. W. Gymer, *Synth. Met.* **2000**, *110*, 1.
[45] M. Campoy-Quiles, T. Ferenczi, T. Agostinelli, P. G. Etchegoin, Y. Kim, T. D. Anthopoulos, P. N. Stavrinou, D. D. C. Bradley, J. Nelson, *Nat. Mater.* **2008**, *7*, 158.
[46] E. Verploegen, R. Mondal, C. J. Bettinger, S. Sok, M. F. Toney, Z. Bao, *Adv. Funct. Mater.* **2010**, *20*, 3519.
[47] H. Sirringhaus, P. J. Brown, R. H. Friend, M. M. Nielsen, K. Bechgaard, B. M. W. Langeveld-Voss, A. J. H. Spiering, R. A. J. Janssen, E. W. Meijer, P. Herwig, D. M. de Leeuw, *Nature* **1999**, *401*, 685.
[48] J. Rivnay, R. Noriega, J. E. Northrup, R. J. Kline, M. F. Toney, A. Salleo, *Phys. Rev. B* **2011**, *83*, 121306.
[49] M. L. Chabinyc, M. F. Toney, R. J. Kline, I. McCulloch, M. Heeney, *J. Am. Chem. Soc.* **2007**, *129*, 3226.
[50] Y. Yi, V. Coropceanu, J. L. Brédas, *J. Am. Chem. Soc.* **2009**, *131*, 15777.
[51] M. D. Perez, C. Borek, S. R. Forrest, M. E. Thompson, *J. Am. Chem. Soc.* **2009**, *131*, 9281.
[52] S. Cho, J. H. Seo, S. H. Park, S. Beaupré, M. Leclerc, A. J. Heeger, *Adv. Mater.* **2010**, *22*, 1253.
[53] N. Blouin, A. Michaud, M. Leclerc, *Adv. Mater.* **2007**, *19*, 2295–2300.
[54] D. Y. Kondakov, C. T. Brown, T. D. Pawlik, *SID Symp. Digest Techn. Papers* **2010**, *41*, 43.
[55] D. Y. Kondakov, W. C. Lenhart, W. F. Nichols, *J. Appl. Phys.* **2007**, *101*, 024512.
[56] F. So, D. Kondakov, *Adv. Mater.* **2010**, *22*, 3762.
[57] H. Aziz, Z. D. Popovic, N. Hu, A. Hor, G. Xu, *Science* **1999**, *283*, 1900.
[58] V. V. Jarikov, K. P. Klubek, L. S. Liao, C. T. Brown, *J. Appl. Phys.* **2008**, *104*, 074914.
[59] M. A. Lampert, P. Mark, *Current Injection in Solids*, Academic Press, New York **1970**.
[60] P. Mark, W. Helfrich, *J. Appl. Phys.* **1962**, *33*, 205.
[61] P. W. M. Blom, M. J. M. de Jong, J. J. M. Vleggaar, *Appl. Phys. Lett.* **1996**, *68*, 3308.
[62] M. M. Mandoc, B. de Boer, G. Paasch, P. W. M. Blom, *Phys. Rev. B* **2007**, *75*, 193202.
[63] Y. Zhang, B. de Boer, P. W. M. Blom, *Phys. Rev. B* **2010**, *81*, 085201.
[64] M. M. Mandoc, B. de Boer, P. W. M. Blom, *Phys. Rev. B* **2006**, *73*, 155205.
[65] S. L. M. van Mensfoort, R. J. de Vries, V. Shabro, H. P. Loebl, R. A. J. Janssen, R. Coehoorn, *Org. Electron.* **2010**, *11*, 1408.
[66] S. L. M. van Mensfoort, J. Billen, S. I. E. Vulto, R. A. J. Janssen, R. Coehoorn, *Phys. Rev. B* **2009**, *80*, 033202.
[67] A. J. Campbell, D. D. C. Bradley, D. G. Lidzey, *J. Appl. Phys.* **1997**, *82*, 6326.
[68] Z. Chiguvare, V. Dyakonov, *Phys. Rev. B* **2004**, *70*, 235207.
[69] D. S. Chung, D. H. Lee, C. Yang, K. Hong, C. E. Park, J. W. Park, S.-K. Kwon, *Appl. Phys. Lett.* **2008**, *93*, 033303.
[70] L. Goris, K. Haenen, M. Nesládek, P. Wagner, D. Vanderzande, L. De Schepper, J. D'Haen, L. Lutsen, J. V. Manca, *J. Mater. Sci.* **2005**, *40*, 1413.
[71] T. W. Holcombe, J. E. Norton, J. Rivnay, C. H. Woo, L. Goris, C. Piliego, G. Griffini, A. Sellinger, J.-L. Brédas, A. Salleo, J. M. J. Frechét, *J. Am. Chem. Soc.* **2011**, *133* 12106.
[72] L. Goris, A. Poruba, L. Hod'ákova, M. Vaněček, K. Haenen, M. Nesládek, P. Wagner, D. Vanderzande, L. De Schepper, J. V. Manca, *Appl. Phys. Lett.* **2006**, *88*, 052113.
[73] S. C. B. Mannsfeld, http://code.google.com/p/wxdiff/2011.